Wood Science and Technology
https://doi.org/10.1007/s00226-022-01412-y

ORIGINAL

Dimensional stabilization of wood by microporous silica aerogel using in-situ polymerization

Miklós Bak[1] · Ferenc Molnár[1] · Rita Rákosa[2] · Zsolt Németh[2] · Róbert Németh[1]

Received: 16 August 2021 / Accepted: 20 August 2022

Abstract

In this paper, a method for dimensional stabilization of wood through bulk hydrophobization was investigated using a sol–gel process resulting in in-situ formation of microporous SiO_2 aerogel. Two different wood species, beech (*Fagus sylvatica*) and Scots pine (*Pinus sylvestris*) were investigated. The incorporation of microporous silica aerogel inside the cell wall and lumen was verified by scanning electron microscopy, energy dispersive spectrometry and Fourier-transform infrared spectroscopy. A leaching test using paper as model material proved the bonding of the aerogel to the cellulose component of the cell wall, which indicates a long-lasting effect of the treatment. The modification of wood with silica aerogel significantly improved its hygroscopicity and dimensional stability, decreased the equilibrium moisture content and water uptake beside a low weight percent gain. Permeability was reduced as a result of the silica aerogel deposition in the macro- and micropores of the modified wood. The treatment resulted in an obvious colour change as well.

Introduction

Investigating the improving effect of nanoparticles and structures on the dimensional stability of wood is an emerging topic nowadays. Furthermore, the utilization of nanostructures to improve various wood properties also is well known. It is possible to achieve low moisture uptake, higher mechanical properties and durability, good UV-protection or fire resistance (Mahltig et al. 2008; Niemz et al. 2010; Yu et al. 2011; Sahin and Mantanis 2011; Rassam et al. 2012; Shabir Mahr et al. 2012).

The use of different organic or inorganic silicon formulations is a well-known method for wood modification. In most cases improved dimensional stability,

✉ Miklós Bak
bak.miklos@uni-sopron.hu

[1] Faculty of Wood Engineering and Creative Industries, University of Sopron, Sopron, Hungary

[2] Spectrometry Laboratory, Ingvesting Team Ltd, Sopron, Hungary

Published online: 02 September 2022

hydrophobicity, fire resistance and durability were reported (Mai and Militz 2004a, b; Pries and Mai 2013). Alkoxysilanes are an obvious solution, as their favourable properties are already shown as hydrophobization agents of various materials, like metals, textiles or glass (Bai et al. 2016; Christodoulou et al. 2013; Dey and Naughton 2016; Przybylak et al. 2016; Rodriguez et al. 2016). It has already been proven that they can improve some important wood properties (decay resistance, hydrophobization) and they are non-toxic (Terziev et al. 2009; Panov and Terziev 2009; Broda and Mazela 2017; Giudice et al. 2013; De Vetter et al. 2009; Wang et al. 2011). Additionally, they might be used as a stabilizing agent for archaeological waterlogged wood material (Broda and Mazela 2017; Broda et al. 2018). One of the most commonly used alkoxysilanes is tetraethoxysilane (TEOS) that is used for aerogel production besides its several other utilizations (Ogiso and Saka 1993; Saka et al. 1992, 2001).

Silica aerogels are porous materials with low density and a high surface area. Its typical nanoscale morphology consists of silica nanoparticles in an open porous 3D particle network. This specific hierarchical structure ensures the material's outstanding physical properties, such as low bulk density (typically 0.05–0.3 g/cm^3) (Reim et al. 2005), high porosity (> 90%) and low thermal conductivity and flammability. Besides, it is possible to modify its surface chemistry to achieve specific properties of superhydrophobic or oleophobic surfaces (Gurav et al. 2010; Pierre and Pajonk 2002; Riffat and Qiu 2012; Hasan et al. 2017; Maleki et al. 2014).

Silica aerogels are regularly used to improve the fire resistance and thermal insulation of glass, cement-based composites, fibre-reinforced composites and wood (Sedighi Gilani et al. 2016b; Lee et al. 2018; Li et al. 2016, 2017; Jaxel et al. 2017; Zeng et al. 2018; Liu et al. 2018; Cotana et al. 2014; Cai et al. 2012). Recently, using silica aerogels in combination with cellulosic materials at the nano and micro scale is mainly done to synthesize high-performance insulation materials to produce new generation building solutions (Demilecamps et al. 2015; Zhao et al. 2015; Sedighi Gilani et al. 2016a). Another focus is on improving the wood and wood-based composites' fire resistance, durability, mechanical properties or reducing moisture and water uptake using mainly different silicon alkoxides and silicon alkoxide derivatives as basic precursors of aerogels (Saka et al. 1992; Saka and Ueno 1997; Zhu et al. 2014; Miyafuji et al. 1998; Miyafuji and Saka 2001; Donath et al. 2006, 2007; Palanti et al. 2012; Shabir Mahr et al. 2012; Unger et al. 2013; Lu et al 2014; Rosenthal and Bues 2010).

Favourable properties of wood modifications by various silicon compounds like improved dimensional stability and durability are coupled with high weight percent gains, usually between 20 and 60% (Donath et al. 2004). Lu et al. (2014) achieved 40–50% reduction in equilibrium moisture content (EMC) besides a 25–30% weight percent gain (WPG) using an ultrasonic-assisted sol–gel method that provided higher efficiency of the treatment. Unger et al. (2013) showed that the ratio of the alkoxysilane and water in the sol is a crucial factor during the gel formation. They concluded that high WPG values do not necessarily result in improved dimensional stability or low EMC. The most important factors are size and reactivity of the particles in the sol. Wood species are an influencing factor on the efficiency of silica-based treatments. Different anatomical structures of different wood species affect the efficiency

of the impregnation process, and thus, the efficiency of the treatments (Götze et al. 2008). Improved hydrophobicity of the wood material was also reported by using WPG values of 15–30% using nano silica sol as a precursor. Water contact angles of 75–80° were achieved with this method (Xu et al. 2020).

Beside the in-situ formation of aerogels in the wood tissue through a sol–gel process it is possible to use aerogel powders as modifying agents. With this process, superhydrophobic poplar veneer was produced with the contact angle of 153°. Additionally, studies on wood modification using "nano-SiO_2" coating techniques on the cell walls are well known to produce highly hydrophobic surfaces with low water and moisture uptake (Wang et al. 2013; Ebrahimi et al. 2017; Bak et al. 2018). When using silica nanoparticles to improve the dimensional stability and hydrophobicity of wood, it is appropriate to use a bonding agent or layer to ensure good fixation of the nanoparticles in the wood, or it is necessary to use an additional hydrophobization step for the treatment (Bak et al. 2018; Wang et al. 2013). Thus, these treatment systems are more complicated compared to the one step methods based on in-situ aerogel formation.

This work shows a simple method of in-stiu sol–gel synthesis of porous silica aerogel inside the cellular structure of wood, using TEOS as a precursor. This study aims to develop a simple method that can improve dimensional stability and reduce water adsorption capacity of the treated wood material using low WPG values compared to other silica treatments. The effects of silica aerogel on wood-water relations in different anatomical directions have also been investigated in detail. As a potential building material, it also is important to study the main diffusion characteristics in different anatomical directions, as well as the colour change as a result of the treatment. The efficiency of the chemical fixation of silica aerogels in the cellulose structure was tested by a leaching process. Since the hydrolysis of wood extractives can distort the results of FTIR spectroscopy, paper was used as a model material in the leaching experiments.

Experimental

Materials

Wood samples of beech (*Fagus sylvatica*) and Scots pine sapwood (*Pinus sylvestris*) originating from the southwestern regions of Hungary were cut into blocks of $20 \times 20 \times 30$ mm (radial × tangential × longitudinal) and $10 \times 50 \times 50$ mm (radial/tangential × tangential/radial × longitudinal). The initial moisture content of the wood was $12 \pm 2\%$. The investigated wood species were chosen because they can be easily impregnated and because of their importance in the wood industry, with increasing needs for outdoor uses as well. Tetraethoxysilane (TEOS) and hydrochloric acid (HCl, 36–38%) were obtained from Sigma-Aldrich Co. LLC, ethanol (ET, 99.99%) was purchased from Merck KGaA, while distilled water (H_2O) was prepared in the laboratory. All chemicals were used as received without further purification.

Preparation of microporous silica aerogel

The SiO_2 aerogel with a porous network structure was prepared by the sol–gel method. The TEOS/ET/H_2O mixture with a molar ratio of 1:5:8 was added into the reaction system. To promote the hydrolysis process, HCl was added dropwise until the pH value reached the value of 3. TEOS/HCl molar ratio of 0.001 was used. The mixture solution was stirred at 500 rpm at 50 °C for 60 min, until the initially opaque solution turned clear.

Preparation of microporous silica aerogel treated samples

All wood samples were oven dried at 105 °C in a drying chamber (Memmert UP 500) prior to the impregnation process for 24 h. The treatment consisted of a 60-min vacuum phase under 100 mbar pressure in a vacuum dryer (Memmert VO 400) at 25 °C and an impregnation step under atmospheric pressure, where the samples were kept in the treatment solution for 120 min. No overpressure was necessary, as small samples were used (20 × 20 × 30 mm for swelling and EMC tests, 10 × 50 × 50 for the water uptake test). The impregnated specimens were then placed in an oven at 60 °C for 24 h, followed by another 24 h at 105 °C to age the gel until SiO_2 aerogel formed in the wood structure.

Test methods

Weight percent gain (WPG)

The increase in weight as a result of the treatment was determined by weighing the samples before the impregnation (ovendry weight, MC = 0%), directly after the impregnation (wet weight), and after the curing step (ovendry weight, MC = 0%) with the accuracy of 0.01 g. WPG was calculated according to Eq. (1):

$$\mathrm{WPG}_{W/D} = \frac{m_{\mathrm{wet}/0,\mathrm{imp}} - m_0}{m_0} \times 100\,[\%] \tag{1}$$

where WPG_W: wet WPG, mass intake of the samples as a result of impregnation with the silica sol (%); WPG_D: dry WPG, mass intake of the samples after gel formation (%); m_{wet}: weight of samples after impregnation with silica sol (kg); $m_{0\mathrm{imp}}$: dry weight of samples after impregnation and gel formation (kg); m_0: dry weight of samples before impregnation with silica sol (kg).

Microscopic analysis

The location and distribution of the silica aerogel in the structure of the wood were investigated by scanning electron microscope (SEM) imaging (Hitachi S3400N). Accelerating voltage of 20 kV was used. The surfaces were coated with a sputter-coater prior to the imaging. 5 × 5 × 5 mm samples from the middle part of the treated material were cut. Longitudinal (radial or tangential) sections were

used for this purpose. The elemental composition was determined on cross sections by regional analysis using an energy dispersive X-ray spectrometer (EDX) combined with SEM (Bruker XFlash Detector 5010). The accelerating voltage was 30 kV. The silicon element mapping was performed on a selected area of 120×80 µm with a spatial resolution of 0.1 µm.

FTIR analysis

ATR reflection spectrometry allows rapid and non-destructive examination of wood. FTIR measurements were performed on the tangential surfaces of the wood samples using a Shimadzu IRAffinity-1 spectrometer equipped with the HATR 10 total reflection accessory kit. The spectra were recorded in the wavenumber range of 4000–670 cm^{-1} with a spectral resolution of 1 cm^{-1} using the Happ-Genzel apodisation. All the spectra were corrected to the background spectra at ambient conditions and the registered spectra were derived from 49 scans.

Various data pre-processing methods were used to eliminate spectral variability caused by surface roughness, inhomogeneity and scattering effects. Firstly, atmospheric correction was used on the spectra to reduce the influences of CO_2 and air humidity (Shimadzu IRsolution 1.60 software). Afterwards, the noise amplitude was reduced by smoothing of the spectra to resolution of 10 cm^{-1}. Ultimately, the SNV (standard normal variate) transformation was performed as a normalization method. The FTIR spectra of wood samples are very complex due to the overlapping absorption of the main components. Using a multivariate data analysis method allows the uncovering of the hidden information content of complex light absorption peaks (Chen et al. 2010). After pre-treatments done, the spectra were assessed by principal component analysis (PCA). PCA decompositions were carried out by the extension Chemometrics Ad-In in Microsoft Excel.

Leaching test

The efficiency of the fixation of silica aerogels in the cellulose macrocomponent was tested by a leaching process. Wood is a complex lignocellulosic material, and the hydrolysis of wood extractives can distort the results of FTIR spectroscopy (Schwanninger et al. 2011). Therefore, paper was used as a model material in the experiments. Paper sheets with the dimensions of 10×100 mm were vacuum impregnated and cured with the same process as used for wood blocks. Leaching of the paper was done by using distilled water or ethanol (99.99%). The first step of the leaching procedure was a 15-min vacuum phase under 100 mbar pressure in a vacuum dryer (Memmert VO 400) at 25 °C, followed by a 120-min impregnation step under atmospheric pressure, by leaving the samples in the leaching agent. The paper specimens were then dried in an oven at 105 °C for 12 h. After this leaching process, FTIR analysis was used to investigate the fixation of the silica aerogel on the cellulose component.

Water repellency

To examine water repellency, contact angle (CA) of deionized water (surface tension: 3.2 mN/m) was evaluated as the ability of the resulting wooden surfaces to repel water. An optical goniometer (68–76 PocketGoniometer PGX+) was used to measure the CA of droplets on the prepared surfaces. Each droplet was dropped onto the sample surface by vibrating the syringe. The volume of the droplet was controlled at around 4 µL. The CA was measured at intervals of 120 ms for the 1st s and at 5, 10, 20, 30, 60, 120, 240, 360, 480 and 570 s. Five samples were used for each type of material. At least 5 CA determinations were made at different locations on the surface of each specimen.

Anti–swelling–efficiency (ASE) and swelling anisotropy

Anti-swelling-efficiency was determined by the measurement of linear swelling in radial and tangential directions on samples with the dimensions of 20 × 20 × 30 mm (radial × tangential × longitudinal). Twenty pieces were used for both wood species, and twenty pieces of untreated samples for both wood species served as the control. The samples were dried at 105 °C until a constant mass was reached and then the dimensions were measured. Subsequently, the samples were soaked in water for 10 days. Finally, the dimensions were measured again.

ASE was determined according to Eq. (2):

$$\mathrm{ASE}_{r,t} = \frac{S_{U,r,t} - S_{T,r,t}}{S_{U,r,t}} \times 100\,[\%] \tag{2}$$

where $\mathrm{ASE}_{r,t}$: anti swelling efficiency, radial or tangential (%); $S_{U,r,t}$: swelling of untreated samples, radial or tangential (%); $S_{T,r,t}$: swelling of treated samples, radial or tangential (%).

Additionally, swelling anisotropy was calculated from the linear swelling data according to Eq. (3):

$$A_{\mathrm{sw}} = \frac{S_t}{S_r} \tag{3}$$

where A_{sw}: swelling anisotropy; $S_{r,t}$: swelling, radial or tangential (%).

Equilibrium moisture content (EMC)

Equilibrium moisture content (EMC) was determined on samples with the dimensions of 20 × 20 × 30 mm (radial × tangential × longitudinal). Ten pieces of each treated and untreated samples were used for both wood species. The samples were dried at 105 °C until constant mass and then weighed. Subsequently, the samples were climatized under constant conditions (20 °C and 65% relative humidity). During this process, the samples were weighed every week. The climatization was

stopped when the difference between two following weights was less than 1% in all control and treated samples. Thus, climatization was stopped after 10 weeks. EMC was determined according to Eq. (4):

$$\mathrm{EMC}_{20/65} = \frac{m_u - m_0}{m_0} \times 100[\ \%] \tag{4}$$

where $\mathrm{EMC}_{20/65}$: equilibrium moisture content of samples at 20 °C and 65% relative humidity (%); m_u: wet weight of the samples after 10 weeks of climatization (g); m_0: dry weight of the samples (g).

Water uptake

Water uptake was determined on samples with the dimensions of 10 × 50 × 50 mm (radial/tangential × tangential/radial × longitudinal) using clear radial or tangential surfaces, to test the water uptake in radial and tangential directions. Ten samples were investigated for each wood species and anatomical direction (radial or tangential) for treated and untreated material as well. Samples were climatized at 20 °C and 65% relative humidity until a constant mass was reached. After climatization, the samples were sealed at the edges and at one radial/tangential surface by a commercial silicon sealant (Soudal neutral silicone). After polymerization of the sealant, samples were weighed and then immersed in distilled water with the unsealed surface facing down and weighed again after 72 h. The water uptake was calculated according to Eq. (5):

$$W = \frac{m_u - m_0}{A} \left[\frac{g}{m^2}\right] \tag{5}$$

where W: water uptake of the samples; m_u: mass of the samples after immersion in water (g); m_0: mass of the samples before immersion in water (g); A: radial or tangential surface area of the samples (m^2).

Water vapour diffusion

The density of water vapour flow rate was measured with the dry-cup test (EN ISO 12572-2016). Untreated specimens served as a control. Specimens were tested for each treated and control wood species, in both tangential and radial directions. Samples were climatized at normal climate ($T = 20$ °C, $\varphi = 65\%$) prior to the test until they reached equilibrium moisture content. The samples were 10 mm thick, with a diameter of 90 mm. The thickness and the diameter of the samples were measured on three points, to have an average thickness and diameter, because of their relatively large surface. The samples had a clear radial or tangential surface. The gap between the specimen and the testing cup was sealed with an acryl-based sealant. Water-free calcium-chloride was used as a desiccant to ensure the 0% relative humidity (RH) in the testing cup. The testing cups were placed in a climatic chamber at 20 °C temperature and 65% RH. Cups were weighed once a day to determine

the mass of the moisture transport through the wood specimens. The density of the water vapour flow rate was calculated according to Eq. (6):

$$g = \frac{G}{A}\left[\frac{\text{kg}}{\text{m}^2\text{s}}\right] \tag{6}$$

where g: density of water vapour flow rate; G: the change of mass per time for a single determination (water vapour flow rate) (kg/s); A: the exposed area of the test specimen (m^2).

Total colour change (Δ*E**)

Colour was measured by a Konica-Minolta 2600d spectrophotometer using CIELab colour coordinates. Measurements were taken using the D65 illuminant and 10° standard observer with a test-window diameter of 8 mm. The relatively large diameter was chosen in order to eliminate as much as possible the natural variability of the colour of the wood. The radial surfaces of climatized samples for water uptake tests were used for colour measurement before and after impregnation, where 3 randomly chosen points were measured on each sample. The total colour change (ΔE*) was calculated according to Eq. (7):

$$\Delta E^* = \sqrt{\Delta L^2 + \Delta a^2 + \Delta b^2} \tag{7}$$

where ΔL: change in lightness as a result of the treatments; Δa: change in red hue as a result of the treatments; Δb: change in yellow hue as a result of the treatments.

Statistical analysis of the results

Distribution normality of the data (WPG, ASE, EMC, water uptake, swelling anisotropy, water vapour diffusion, total colour change) was verified and statistical significance tests (ANOVA, Fischer LSD-test, $p < 0.05$) were conducted for the effect of the treatment on the investigated material properties with the software Statistica 10.0 (Statsoft).

Results and discussion

Weight percent gain

There were significant differences in the dry and wet WPG of the examined wood species. Variation coefficients of the WPGs of beech samples were significantly lower. This result shows a more even impregnation level (measured by quantity) of beech material, which is not necessarily equal to the even distribution of aerogel in the wood tissue. However, the mean value of the WPG of pine samples was higher. The ratio of dry and wet WPG was 8.71 and 9.29% for beech and pine, respectively (Table 1). This indicates that the penetration of the silica compound

Table 1 WPG values of beech and pine samples as a result of porous silica aerogel treatment

	Beech		Pine	
	WPG_{wet} (%)	WPG_{dry} (%)	WPG_{wet} (%)	WPG_{dry} (%)
Mean	79.22	6.90	101.14	9.40
Min	65.61	5.53	71.38	6.00
Max	94.82	9.01	130.50	11.99
St. Dev	7.94	1.03	20.17	2.25
Var. Coeff	10.02%	14.92%	19.94%	23.89%

and the process of gel formation were not influenced by the wood species. Thus, the characteristics of impregnation did not affect the results. The WPG obtained with this treatment is rather low (6.9% and 9.4% for beech and pine, respectively), compared to some other silica-based modification methods, where usually 20–60% WPG is reported (Donath et al. 2004). It fits with the goal of the research to keep the WPG low, to improve the wood properties by using only a low amount of the modification agent. The molar ratio of TEOS in the silica sol was only 7.14%, so this result corresponded to the expectations of keeping the WPG low.

SEM imaging

Aerogel mostly forms a uniform, thin coating on the surface (Fig. 1a–c). This aerogel coating on the cell wall surfaces was often fragmented, showing cracks (Fig. 1b, c). Thus, the continuity of the aerogel coating was terminated. The reason for cracking is the shrinkage of the aerogel during the drying and curing process of the treatment, because of the high solvent ratio of the treatment system (TEOS/ET/H_2O molar ratio of 1:5:8). Beside the coating effect, larger deposits, agglomerations in the cell lumens of fibres, tracheids and rays were found as well (Fig. 1b). This indicates that the amount of TEOS in the treatment system was more than enough to efficiently cover the cell wall surfaces with aerogel. This result fits with the goal to keep the amount of aerogel low in the wood. However, this kind of deposit in the cell lumen might decrease water uptake by clogging the lumens, as the silica aerogel agglomerations in the cell lumen prevent further penetration of water, resulting in improved dimensional stability (Götze et al. 2008).

The porous structure of the aerogel was better visible in the deposits (Fig. 1c). Aerogel backbones are built from spherical blocks. The determination of the diameters of the globules is difficult because they overlap in the image. A rough estimation gives a globule size between 75 and 150 nm. The majority of pores are in the micropores (0.2–2 nm) range, although some mesopores (2–50 nm) can also be seen in the images. However, in some deposits, macropores (50–1000 nm) are visible as well. The presence of different pore size in silica aerogels is reported by other authors as well (Veres et al. 2017; Rahmani et al. 2018; Faghihian et al. 2013).

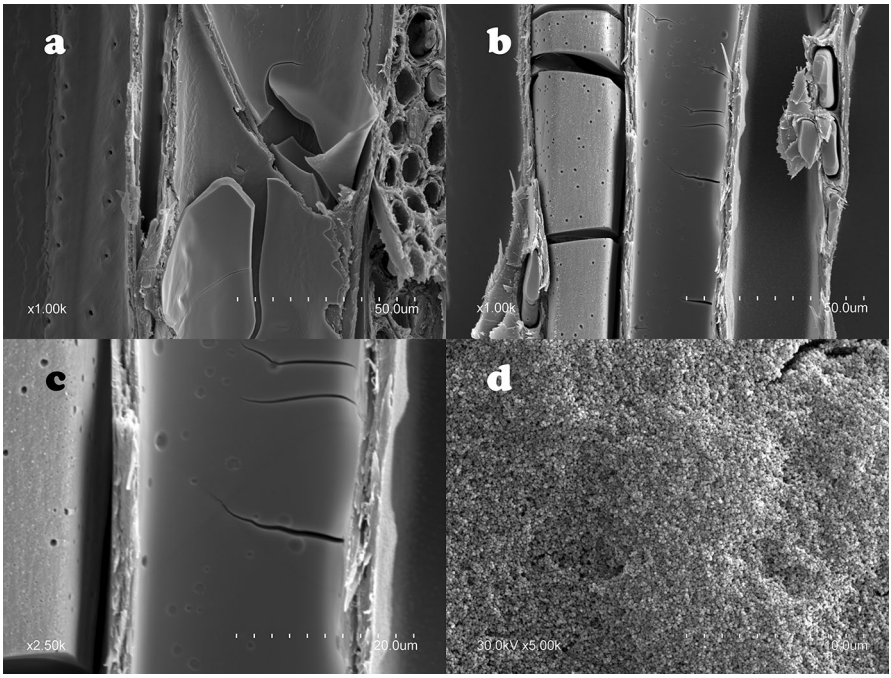

Fig. 1 SEM images of the aerogel impregnated wood material showing (**a**) the thin coating on the cell wall surface, (**b**) agglomerations in the cell lumen, (**c**) cracks in the aerogel coating, and (**d**) the microporous structure of the silica aerogel

EDX analysis

Parallel to the SEM imaging, the EDX analysis of the samples was done to get more detailed information about the location and the distribution of the aerogel. These results supported the data from SEM imaging, as it showed the presence of silica

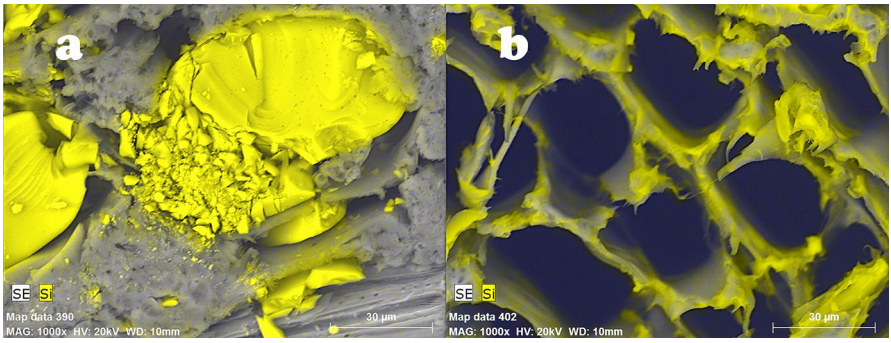

Fig. 2 EDX maps of aerogel treated beech wood showing agglomerations in the cell lumens (**a**) and its distribution (**b**)

particles in the cell wall and on its surface, beside some agglomerations (Fig. 2a, b.). This means that SiO_2 aerogel can remain in the wood since wood itself does not have so much Si element. As the samples were obtained 3 mm from each radial, tangential, and transverse surface of the wood, SiO_2 sol can easily be inserted into the beech and pine wood.

FTIR analysis

FTIR spectra reflect the chemical composition of wood samples. The characteristic light absorption peaks are provided by the stretching and deformation vibrational transitions of the functional groups and aromatic/conjugated and unsaturated moieties. Although, the spectra were collected in the region between 4000 and 670 cm^{-1}, data evaluation was limited to the fingerprint region (1800–800 cm^{-1}), where most of the absorption bands characterizing the sample quality occurred. Absorption bands were assigned based on the literature (Pandey and Pitman 2003; Gwon et al. 2010; Yue et al. 2019; Báder et al. 2020). The absorption peak at 1730 cm^{-1} can be associated with the C=O stretching vibration in the hemicellulose. The bands at 1592 cm^{-1} and 1503 cm^{-1} correspond to vibrations in the aromatic rings of lignin. The peaks located at 1368, 1422 and 1458 cm^{-1} were attributed to the C-H deformation in polysaccharides and lignin. The peaks observed in the range 900–1200 cm^{-1} were assigned to the C–O–C vibration and C–H, C–O deformation in carbohydrates. The small differences between the SNV transformed spectra of beech and pine wood are due to the differences in the chemical composition of these wood species (Fig. 3).

The absorption peaks in the spectrum of treated wood observed at 1079 and 789 cm^{-1} correspond to the asymmetric stretching vibration and bending mode of Si–O–Si (Fig. 3) (Gwon et al. 2010; Fu et al. 2016; Yue et al. 2019). They show that the TEOS on the wood surface were hydrolysed. Then, during the polycondensation reaction, a cross-linked gel was formed with the formation of siloxane bonds. The FTIR spectra indicate the change in the chemical properties of the wood surface

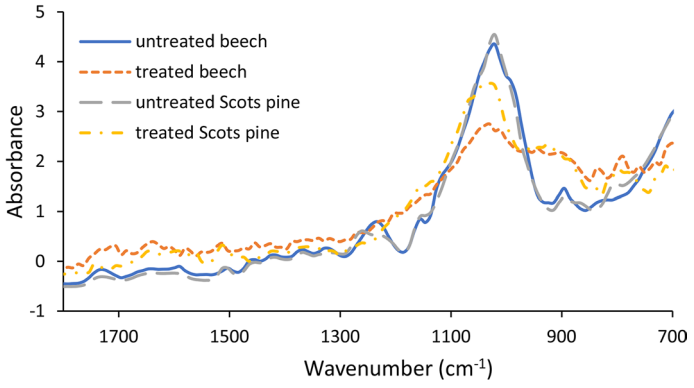

Fig. 3 SNV transformed FTIR spectra of untreated and treated Scots pine sapwood and beech wood

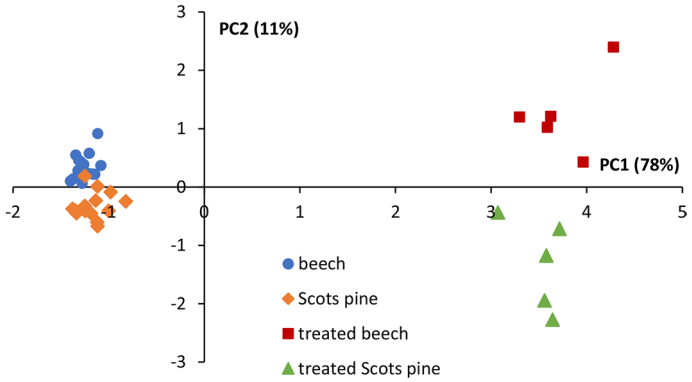

Fig. 4 PCA score plot for the control and treated wood samples in the 1800–800 cm^{-1} spectral region

after modification. The reactions that take place during the process are as follows (Yue et al. 2019):

$$\mathrm{Si}\left(\mathrm{O}-\mathrm{CH_2}-\mathrm{CH_3}\right)_4 + 4\,\mathrm{H_2O} \rightarrow \mathrm{Si(OH)_4} + 4\,\mathrm{CH_3}-\mathrm{CH_2}-\mathrm{OH} \quad n\,\mathrm{Si(OH)_4} \rightarrow n\,\mathrm{SiO_2} + 4n\,\mathrm{H_2O}$$

Principal component analysis is commonly used to reduce the dimensionality of the spectral data. By using PCA, new and linearly uncorrelated variables (principal components) are generated by transformation on a matrix containing the spectral data of the samples. The data points can be represented graphically in a two-dimensional subspace that is defined by the first and second principal components (PC1 and PC2). The similarities or differences between the samples are expressed by their relative distances from each other. Performing PCA decomposition on the spectra enabled the discrimination between soft- and hardwood samples and between untreated and treated wood samples (Fig. 4). The PC1 axis represents the treatment, while the PC2 axis integrates differences in the chemical structure between wood species. The discrimination of the samples is due to the change in the chemical composition of the wood, and distances from the centroids give some information about the magnitude of the molecular changes.

The change in the FT-IR spectra of the impregnated paper with or without leaching by ethanol and water is shown in Fig. 5.

The similarity of the spectra can be characterized by the linear regression patterns of the SNV transformed spectrum pairs, and of course, by the R^2 values pertaining to them. The SNV spectra perfectly fitting to each other are able to define a straight regression line with a unit slope and zero intercept and $R^2 = 1$ value. Based on this simply statistical concept, the spectra obtained after the leaching process were established to be equivalent to those of the impregnated sample (Fig. 6). Thus, the silica aerogel is chemically able to bond to the cellulose macro component efficiently.

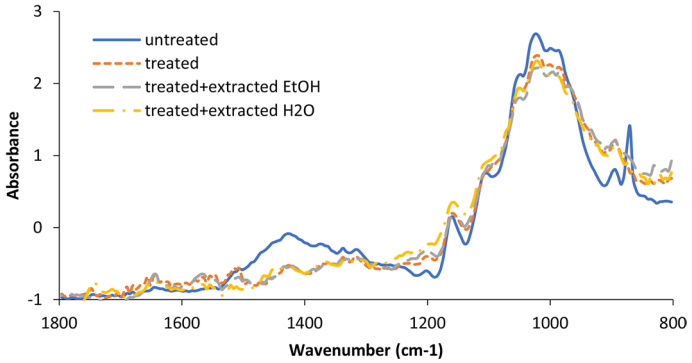

Fig. 5 SNV transformed FTIR spectra of the impregnated paper with or without leaching by ethanol and water

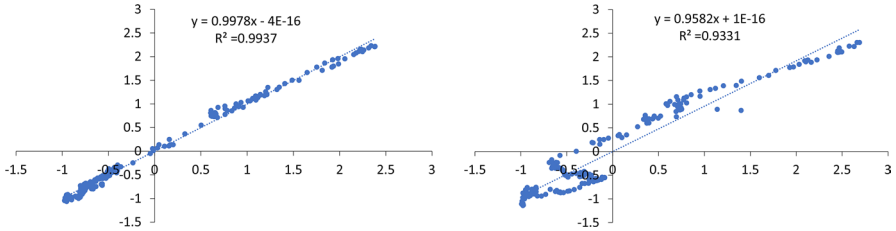

Fig. 6 **a** Similarity between the SNV spectra of impregnated and impregnated + extracted samples. **b** Similarity between the SNV spectra of control and impregnated + extracted samples

Water repellence

Results showed a high hydrophobization effect as a result of the investigated silica-based treatment (Fig. 7). The initial contact angle (at time = 0 s) of the untreated wood material was around 65–70° for both wood species. In contrast to that, significantly higher contact angles were observed for the SiO_2 aerogel treated wood surfaces, between 130 and 135°. This is close to the superhydrophobic region (> 150°). The treatments not only provide high hydrophobicity for wood, but they also provide a long-lasting effect, as the contact angle only slightly decreases with time. Thus, the microporous silica aerogel treatment is a stable treatment. These results support the conclusions of the dimensional stabilization and water uptake decreasing effect of the treatments. One of the main reasons, why these treatments improve these properties of wood is the long-lasting hydrophobization effect of the treatments.

Anti-swelling-efficiency (ASE) and swelling anisotropy

Shrinking and swelling was decreased remarkably by the aerogel treatment in beech and pine (Fig. 8). Silica aerogel treatment resulted in a slightly, but significantly lower ASE in both the radial and tangential directions in pine wood (35.17% and

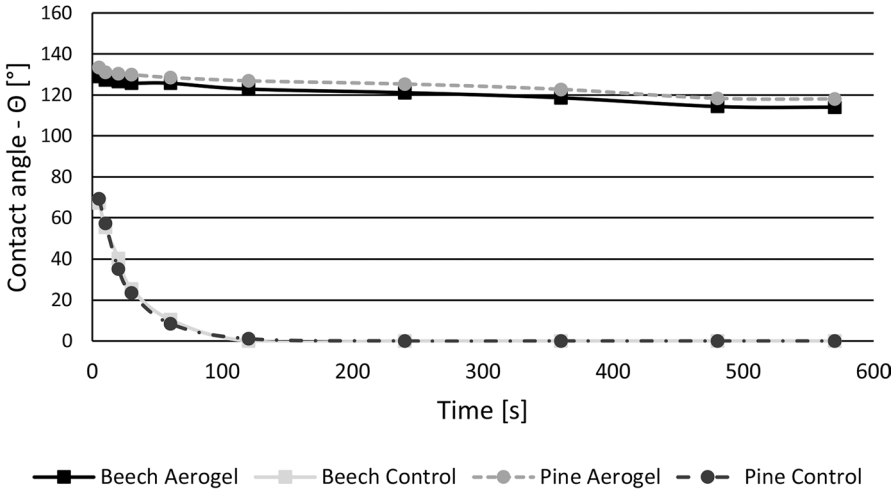

Fig. 7 Effect of silica aerogel treatment on the contact angle of beech and Scots pine wood

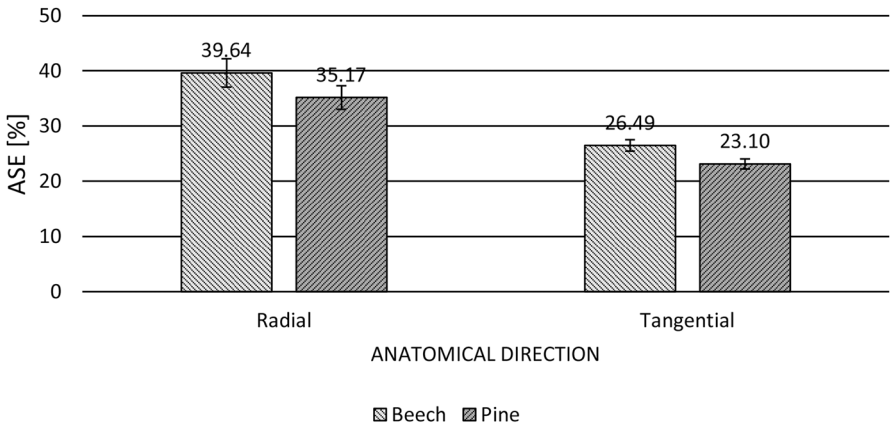

Fig. 8 ASE of silica aerogel treatment of beech and Scots pine wood (whiskers show standard deviation of the results)

23.10%, respectively), compared to beech (39.64% and 26.49%, respectively). Wood species has only a moderate effect, resulting from the different anatomical structures, which is responsible for different permeability.

The ASE is relatively high, beside using a low amount of silica aerogel as a modifying agent. According to the ASE results, the affinity of water for the cell wall components decreased. Silica aerogel is responsible for a permanent bulking of the cell wall, as the available space for water molecules decreased (Wang et al. 2013; Tshabalala et al. 2003). Additionally, a chemical reaction between the cell wall molecules and the silica compounds blocked the functional groups responsible for bonding water (Fig. 3.). Another reason for the low water uptake is the reduced

hygroscopicity (Kumar et al. 2016) because of the treatment, proved by a water contact angle of 130–135° (Fig. 7). All these effects contributed to the increase in dimensional stability. Additionally, the aerogel covered the cell wall surface, that delays and prevents the penetration of water molecules to the cell wall as well. Higher WPG values of pine (Table 1) did not result in higher ASE values in either the radial or tangential directions.

Various authors reported an ASE between 8 and 69% using different alkoxysilanes (tetraethoxysilane, propyl triethoxysilane, methyl triethoxysilane, diethyldiethoxysilane, ethyltriethoxysilane) as precursors for silane-based wood modification processes (Donath et al. 2004; Furuno et al. 1992). In these cases, WPG between 16 and 65% was used, while in the investigated silica aerogel treatment, an ASE of 23–40% was achieved at a WPG of 6.9% and 9.4% for beech and pine, respectively.

ASE was significantly different in the radial and tangential directions. This difference slightly increased the swelling anisotropy (Fig. 9). Higher swelling anisotropy promotes cracking, warping and deformations of wood used outdoors, under changing environmental conditions. The ratio of the swelling in radial and tangential directions is below the value of 2, which is the theoretical upper limit that is considered to be a low or moderate capability of wood for deformations and warping related to the changes in the moisture content of wood (Skaar 1988).

Equilibrium moisture content

A remarkable decrease of 28.46% and 36.44% for beech and pine, respectively, was observed in its EMC, as a result of the investigated silica aerogel treatment (Fig. 10). The uptake of water vapour is decreased as a result of the treatment. The presence of silica aerogel decreases the water vapour uptake and the hydrophobation effect by the exclusion of moisture from the cell wall pores and the cell wall surfaces

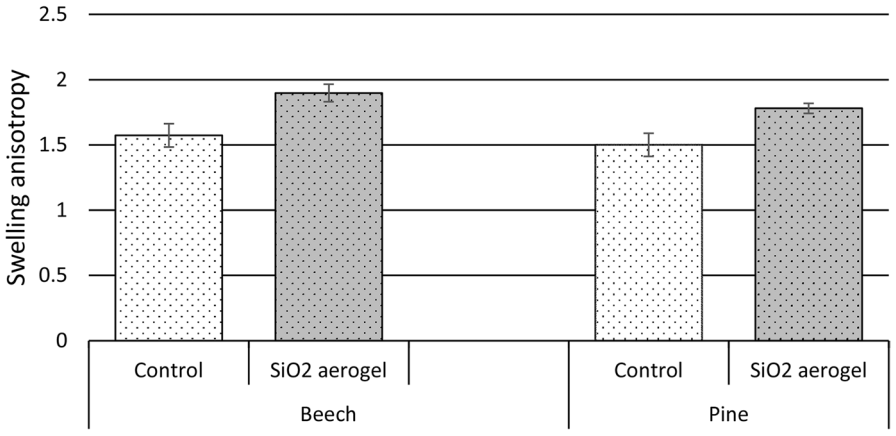

Fig. 9 Effect of silica aerogel treatments on the swelling anisotropy (whiskers show standard deviation of the results)

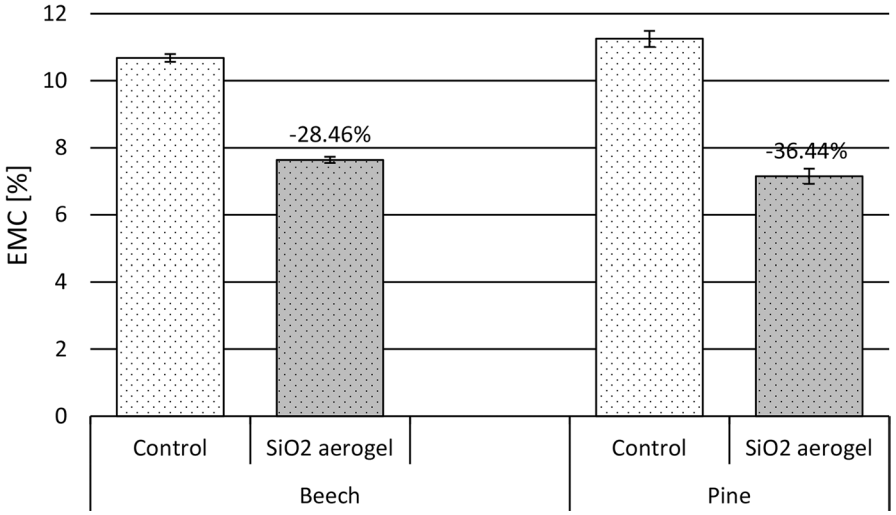

Fig. 10 Effect of silica aerogel treatment on the equilibrium moisture content of beech and Scots pine wood (Percentages show the difference to the control and whiskers the standard deviation of the results)

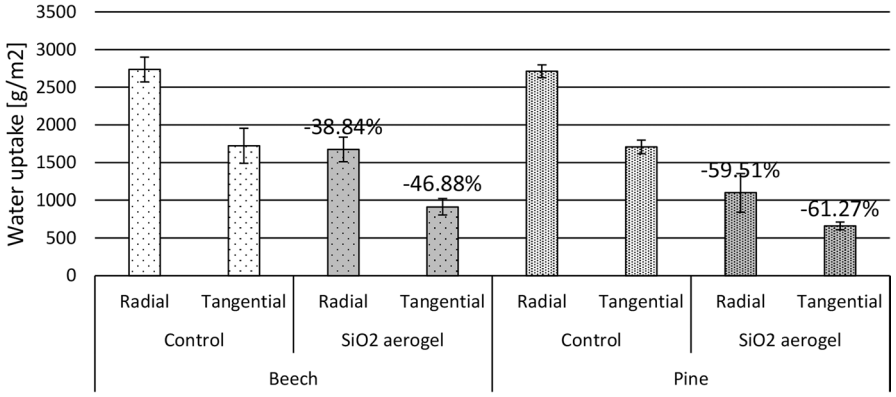

Fig. 11 Effect of silica aerogel treatment on the water uptake of beech and Scots pine wood in radial and tangential directions (Percentages show the difference to the control and whiskers the standard deviation of the results)

(clogging effect) (Kumar et al. 2016). The decrease in EMC was higher in pine wood, which was in accordance with the different WPG values for the wood species.

Water uptake

Water uptake was reduced significantly in both the radial and tangential directions as a result of the treatment (Fig. 11). Accordingly, the cell wall surfaces were covered by an efficient amount of silica aerogel to exclude liquid water from the cell wall (Wang et al. 2013). The penetration of liquid water was hindered by the

blocking of pits and micropores of the cell (Dong et al. 2015). The porous aerogel aggregates that were observed in cell lumens and pores by SEM (Fig. 1b) provided an additional barrier against the penetration of water into the wood tissue (Dong et al. 2015). The aerogel layers and depositions showed a nano-structured surface (Fig. 1d) with increased roughness. This phenomenon further reduced the surface free energy, similar to the lotus effect known from nature (Dong et al. 2015; Neinhuis and Barthlott 1997).

The water absorption always decreased to a greater extent than the equilibrium moisture content. This result supports that beside the lower water uptake capacity, a hydrophobization effect of the microporous silica aerogel treatment is the reason for less water adsorption. This effect explains the different efficiency of the treated material during the adsorption process of liquid water and water vapour.

Water vapour diffusion

Tests showed that the density of water vapour flow rate (g) changed differently in beech and pine wood as a result of the treatment used on wood for dimensional stabilization (Fig. 12). Despite the porous characteristic of the aerogel, a remarkable decrease in the permeability was observed for beech wood, as permeability decreased by 70–80%. However, the WPG of pine samples was higher than that of beech samples, permeability of pine remained unchanged compared to the control. The reason behind the decreased permeability is their polymerization of the treatment system on the cell lumen surfaces, and the presence of agglomerations in the cell lumens, which leads to the inhibition of the water vapour transport through the wood tissue.

One reason for making the wood more water vapour resistant as a result of the treatment can be the decreasing hygroscopicity and equilibrium moisture content.

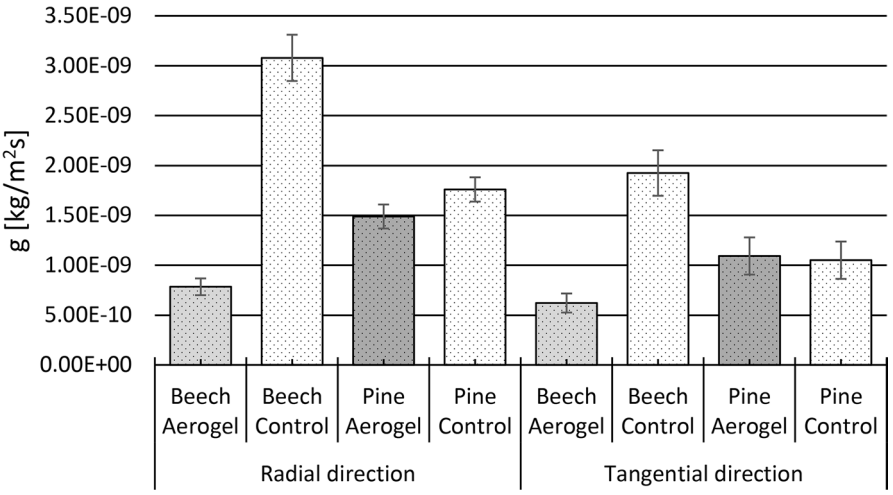

Fig. 12 Effect of silica aerogel treatment on the density of water vapour flow rate of beech and Scots pine wood in the radial and tangential directions (Whiskers show the standard deviation of the results)

These phenomena decrease the moisture content difference between the two surfaces of the wood, which are exposed to different climatic conditions (in this case 0% and 65% RH). Thus, the moisture gradient becomes smaller. On the one hand this slows the moisture diffusion through the wood. On the other hand, as a result of blocking the sorption sites with the aerogel treatment, the distance between the accessible hydroxyl groups in the cell wall will increase which will slow the diffusion as well. The different behaviour of the two wood species can be explained by the different pore proportion of each species. Beech has around 48% pore proportion, while Scots pine about 67% (Wagenführ 1996). Therefore, even a smaller amount of aerogel that clogs the pores and covers the cell wall surfaces might lead to the decrease in the permeability.

Good water vapour permeability is a positive property when wood is used as a building material. Additionally, the treatments did not influence the ratio of water vapour permeability between the radial and tangential directions. As expected, the water vapour permeability was higher in the radial direction, compared to the tangential. This is because of the presence of rays in the radial direction that improve its permeability.

Colour change

The in-situ silica aerogel treatment affected the colour of the samples as a clearly visible darkening (Fig. 13). The total colour change was significantly lower in pine (21.95), compared to beech (33.60) (Fig. 14). The colour change was initiated by the leaching effect of the water and ethanol solvents (especially that of ethanol) used for the in-situ sol–gel process. Another cause was the use of HCl for setting the pH of 3 for the promotion of hydrolytic reactions during the

Fig. 13 Colour change of beech (left) and Scots pine (right) wood material as a result of different silica aerogel treatments

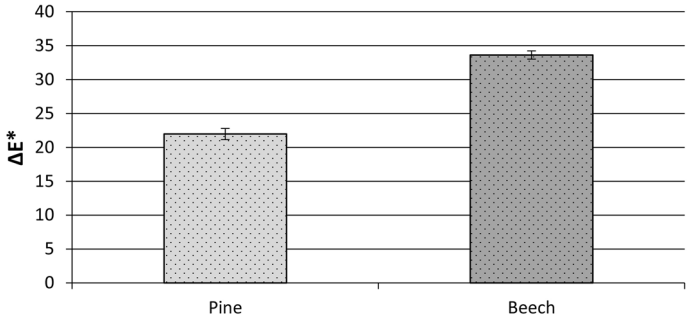

Fig. 14 Total colour change of beech and pine wood material as a result of silica aerogel treatment (Whiskers show standard deviation of the results)

treatment. These effects were amplified by the elevated temperature used for curing the aerogel system (Fan et al. 2010).

Conclusion

With the use of the microporous silica aerogel, it is possible to improve the dimensional stability of wood. Shrinking and swelling properties decreased remarkably, depending on the wood species and anatomical direction. The ASE was similar in the radial and tangential directions for both beech and pine. Swelling anisotropy was increased slightly as a result of a higher ASE in the radial direction, compared to the tangential direction. The improved hydrophobicity of the cell wall surfaces through the deposition of silica aerogel makes these treatments more effective against liquid water, compared to water vapour. However, a remarkable decrease in the permeability of beech wood was observed related to the lower proportion of pores in beech wood.

SEM imaging showed the distribution of the aerogel, as a covering layer on the cell wall surfaces, beside some deposits and agglomerations in the cell lumen However, cracking of the aerogel coating on the cell wall was also observed. EDX mapping showed the presence of the silica aerogel in the cell wall. FTIR measurements proved a chemical bonding of the silica aerogel to the cellulose structure of wood, which indicates a long-lasting effect of the treatment. As a side effect of the treatments, an explicit colour darkening occurred. As a simple method, it might be used as a commercial method in the future. As outdoor use is expected, weathering resistance and durability tests might also be necessary.

Acknowledgements This article was made in frame of the project TKP2021-NKTA-43 which has been implemented with the support provided by the Ministry of Innovation and Technology of Hungary (successor: Ministry of Culture and Innovation of Hungary) from the National Research, Development and Innovation Fund, financed Under the TKP2021-NKTA funding scheme.

Funding Open access funding provided by University of Sopron.

Declarations

Conflict of interest On behalf of all authors, the corresponding author states that there is no conflict of interest.

References

Báder M, Németh R, Sandak J, Sandak A (2020) FTIR analysis of chemical changes in wood induced by steaming and longitudinal compression. Cellulose 27(3):6811–6829. https://doi.org/10.1007/s10570-020-03131-8

Bai Y, Dong Q, Shao Y, Deng Y, Wang Q, Shen L, Wang D, Wei W, Huang J (2016) Enhancing stability and efficiency of perovskite solar cells with crosslinkable silane-functionalized and doped fullerene. Nat Commun. https://doi.org/10.1038/ncomms12806

Bak M, Molnár F, Németh R (2018) Improvement of dimensional stability of wood by silica nanoparticles. Wood Mater Sci Eng 14(1):48–58

Broda M, Mazela B (2017) Application of methyltrimethoxysilane to increase dimensional stability of waterlogged wood. J Cult Herit 25:149–156. https://doi.org/10.1016/j.culher.2017.01.007

Broda M, Majka J, Olek W, Mazela B (2018) Dimensional stability and hygroscopic properties of waterlogged archaeological wood treated with alkoxysilanes. Int Biodeter Biodegr 133:34–41. https://doi.org/10.1016/j.ibiod.2018.06.007

Cai J, Liu S, Feng J, Kimura S, Wada M, Kuga S, Zhang LN (2012) Cellulose-silica nanocomposite aerogels by in situ formation of silica in cellulosegel. Angew Chem 124:2118–2121. https://doi.org/10.1002/anie.201105730

Chen H, Ferrai C, Angiuli M, Yao J, Raspi C, Bramanti E (2010) Qualitative and quantitative analysis of wood samples by Fourier transform infrared spectroscopy and multivariate analysis. Carbohyd Polym 82:772–778. https://doi.org/10.1016/j.carbpol.2010.05.052

Christodoulou C, Goodier CI, Austin SA, Webb J, Glass GK (2013) Long-term performance of surface impregnation of reinforced concrete structures with silane. Constr Build Mater 48:708–716. https://doi.org/10.1016/j.conbuildmat.2013.07.038

Cotana F, Pisello AL, Moretti E, Buratti C (2014) Multipurpose characterization of glazing systems with silica aerogel: in-field experimental analysis of thermal-energy, lighting and acoustic performance. Build Environ 81:92–102. https://doi.org/10.1016/j.buildenv.2014.06.014

De Vetter L, Stevens M, Van Acker J (2009) Fungal decay resistance and durability of organosilicon-treated wood. Int Biodeter Biodegr 63(2):130–134. https://doi.org/10.1016/j.ibiod.2008.08.002

Demilecamps A, Beauger C, Hildenbrand C, Rigacci A, Budtova T (2015) Cellulose–silica aerogels. Carbohyd Polym 122:293–300. https://doi.org/10.1016/j.carbpol.2015.01.022

Dey T, Naughton D (2016) Cleaning and anti-reflective (AR) hydrophobic coating of glass surface: a review from materials science perspective. J Sol Gel Sci Technol 77(1):1–27. https://doi.org/10.1007/s10971-015-3879-x

Donath S, Militz H, Mai C (2004) Wood modification with alkoxysilanes. Wood Sci Technol 38(7):555–566. https://doi.org/10.1007/s00226-004-0257-1

Donath S, Militz H, Mai C (2006) Treatment of wood with aminofunctional silanes for protection against wood destroying fungi. Holzforschung 60(2):210–216. https://doi.org/10.1515/HF.2006.035

Donath S, Militz H, Mai C (2007) Weathering of silane treated wood. Holz Roh Werkst 65(1):35–42. https://doi.org/10.1007/s00107-006-0131-y

Dong Y, Yan Y, Zhang S, Li J, Wang J (2015) Flammability and physical–mechanical properties assessment of wood treated with furfuryl alcohol and nano-SiO_2. Eur J Wood Prod 73(4):457–464. https://doi.org/10.1007/s00107-015-0896-y

Ebrahimi F, Farazi R, Karimi EZ, Beygi H (2017) Dichlorodimethylsilane mediated one-step synthesis of hydrophilic and hydrophobic silica nanoparticles. Adv Powder Technol 28(3):932–937. https://doi.org/10.1016/j.apt.2016.12.022

Faghihian H, Nourmoradi H, Shokouhi M (2013) Removal of copper (II) and nickel (II) from aqueous media using silica aerogel modified with amino propyl triethoxysilane as an adsorbent: equilibrium, kinetic, and isotherms study. Desal Water Treat 52(1–3):305–313. https://doi.org/10.1080/19443994.2013.785367

Fan Y, Gao J, Chen Y (2010) Colour responses of black locust (*Robinia pseudoacacia* L.) to solvent extraction and heat treatment. Wood Sci Technol 44:667–678. https://doi.org/10.1007/s00226-009-0289-7

Fu Y, Liu X, Cheng F, Sun J, Qin Z (2016) Modification of the wood surface properties of *Tsoongiodendron odorum* Chun with silicon dioxide by a sol-gel method. BioResources 11(4):10273–10285. https://doi.org/10.15376/biores.11.4.10273-10285

Furuno T, Shimada K, Uehara T, Jodai S (1992) Combinations of wood and silicate. 2. Wood–mineral composites using water glass and reactance of barium chloride, boric acid, and borax and their properties. Mokuzai Gakkaishi 38:448–457

Giudice CA, Alfieri PV, Canosa G (2013) Decay resistance and dimensional stability of *Araucaria angustifolia* using siloxanes synthesized by sol–gel process. Int Biodeter Biodegr 83:166–170. https://doi.org/10.1016/j.ibiod.2013.05.015

Götze J, Möckel R, Langhof N, Hengst M, Klinger M (2008) Silicification of wood in the laboratory. Ceram Silikáty 52(4):268–277

Gurav JL, Jung I-K, Park H-H, Kang ES (2010) Nadargi DY (2010) Silica aerogel: synthesis and applications. J Nanomater 24:1–11. https://doi.org/10.1155/2010/409310

Gwon JG, Lee SY, Doh GH, Kim JH (2010) Characterization of chemically modified wood fibers using FTIR spectroscopy for biocomposites. J Appl Polym Sci 116(6):3212–3219. https://doi.org/10.1002/app.31746

Hasan MA, Sangashetty R, Esther ACM, Patil SB, Sherikar BN, Dey A (2017) Prospect of thermal insulation by silica aerogel: a brief review. J Inst Eng Ser D 98(2):297–304. https://doi.org/10.1007/s40033-017-0136-1

EN ISO 12572(2016) Hygrothermal performance of building materials and products. Determination of water vapour transmission properties. Cup method. European Committee for Standardization, Brussels

Jaxel J, Markevicius G, Rigacci A, Budtova T (2017) Thermal superinsulating silica aerogels reinforced with short man-made cellulose fibers. Compos Part A Appl Sci Manuf 103:113–121. https://doi.org/10.1016/j.compositesa.2017.09.018

Kumar A, Ryparová P, Škapin AS, Humar M, Pavlič M, Tywoniak J, Hajek P, Žigon J, Petrič M (2016) Influence of surface modification of wood with octadecyltrichlorosilane on its dimensional stability and resistance against *Coniophora puteana* and molds. Cellulose 23(5):3249–3263. https://doi.org/10.1007/s10570-016-1009-8

Lee KJ, Choe YJ, Kim YH, Lee KJ, Hwang HJ (2018) Fabrication of silica aerogel composite blankets from an aqueous silica aerogel slurry. Ceram Int 44:2204–2208. https://doi.org/10.1016/j.ceramint.2017.10.176

Li Z, Gong L, Cheng X, He S, Li CC, Zhang HP (2016) Flexible silica aerogel composites strengthened with aramid fibers and their thermal behavior. Mater Des 99:349–355. https://doi.org/10.1016/j.matdes.2016.03.063

Li C, Cheng X, Li Z, Pan YH, Huang YJ, Gong LL (2017) Mechanical, thermal and flammability properties of glass fiber film/silica aerogel composites. J Non Cryst Solids 457:52–59. https://doi.org/10.1016/j.jnoncrysol.2016.11.017

Liu S, Zhu K, Cui S, Shen XD, Tan G (2018) A novel building material with low thermal conductivity: rapid synthesis of foam concrete reinforced silica aerogel and energy performance simulation. Energy Build 177:385–393. https://doi.org/10.1016/j.enbuild.2018.08.014

Lu Y, Feng M, Zhan H (2014) Preparation of SiO_2–wood composites by an ultrasonic-assisted sol–gel technique. Cellulose 21:4393–4403. https://doi.org/10.1007/s10570-014-0437-6

Mahltig B, Swaboda C, Roessler A, Böttcher H (2008) Functionalising wood by nanosol application. J Mater Chem 27(18):3180–3192. https://doi.org/10.1039/b718903f

Mai C, Militz H (2004a) Modification of wood with silicon compounds. Inorganic silicon compounds and sol-gel systems: a review. Wood Sci Technol 37(5):339–348. https://doi.org/10.1007/s00226-003-0205-5

Mai C, Militz H (2004b) Modification of wood with silicon compounds. Treatment systems based on organic silicon compounds: a review. Wood Sci Technol 37:453–461. https://doi.org/10.1007/s00226-004-0225-9

Maleki H, DurãesL PA (2014) An overview on silica aerogels synthesis and different mechanical reinforcing strategies. J Non-Cryst Solids 385:55–74. https://doi.org/10.1016/j.jnoncrysol.2013.10.017

Miyafuji H, Saka S (2001) Na_2O–SiO_2 wood-inorganic composites prepared by the sol–gel process and their fire-resistant properties. J Wood Sci 47(6):483–489. https://doi.org/10.1007/BF00767902

Miyafuji H, Saka S, Yamamoto A (1998) SiO2–P2O5–B2O3 wood–inorganic composites prepared by metal alkoxide oligomers and their fire-resisting properties. Holzforschung 52:410–416. https://doi.org/10.1515/hfsg.1998.52.4.410

Neinhuis C, Barthlott W (1997) Characterization and distribution of water-repellent, self-cleaning plant surfaces. Ann Bot 79:667–677. https://doi.org/10.1006/anbo.1997.0400

Niemz P, Mannes D, Herbers Y, Koch W (2010) Untersuchungen zum Verhalten von mit Nanopartikeln imprägniertem Holz bei Freibewitterung: (Studies on the behavior of wood impregnated with nanoparticles when exposed outdoors). Bauphysik 32(4):226–232. https://doi.org/10.1002/bapi.201010026

Ogiso K, Saka S (1993) Wood–inorganic composites prepared by sol-gel process: 2: effects of ultrasonic treatments on preparation of wood–inorganic composites. Mokuzai Gakkaishi 39:301–307

Palanti S, Feci E, Predieri G, Vignali F (2012) A wood treatment based on siloxanes and boric acid against fungal decay and coleopter *Hylotrupes bajulus*. Int Biodeter Biodegr 75:49–54. https://doi.org/10.1016/j.ibiod.2012.07.019

Pandey K, Pitman A (2003) FTIR studies of the changes in wood chemistry following decay by brown-rot and white-rot fungi. Int Biodeter Biodegr 52:151–160. https://doi.org/10.1016/S0964-8305(03)00052-0

Panov D, Terziev N (2009) Study on some alkoxysilanes used for hydrophobation and protection of wood against decay. Int Biodeter Biodegr 63:456–461. https://doi.org/10.1016/j.ibiod.2008.12.003

Pierre AC, Pajonk GM (2002) Chemistry of aerogels and their applications. Chem Rev 102(11):4243–4265. https://doi.org/10.1021/cr0101306

Pries M, Mai C (2013) Fire resistance of wood treated with a cationic silica sol. Eur J Wood Prod 71:237–244. https://doi.org/10.1007/s00107-013-0674-7

Przybylak M, Maciejewski H, Dutkiewicz A, Dąbek I, Nowicki M (2016) Fabrication of superhydrophobic cotton fabrics by a simple chemical modification. Cellulose 23(3):2185–2197. https://doi.org/10.1007/s10570-016-0940-z

Rahmani A, Nazemi F, Barjasteh-Askari F, Davoudi M (2018) Preparation, characterization, and application of silica aerogel for adsorption of phenol: an in-depth isotherm study. Health Scope 7(3):e15115. https://doi.org/10.5812/jhealthscope.15115

Rassam G, Abdib Y, Abdia A (2012) Deposition of TiO_2 nano-particles on wood surfaces for UV and moisture protection. J Exp Nanosci 7(4):468–476. https://doi.org/10.1080/17458080.2010.538086

Reim M, Korner W, Manara J, Korder J, Arduini-Schuster M, Ebert HP, Fricke J (2005) Silica aerogel granulate material for thermal insulation and daylighting. Sol Energy 79(2):131–139. https://doi.org/10.1016/j.solener.2004.08.032

Riffat SB, Qiu G (2012) A review of state-of-the-art aerogel applications in buildings. Int J Low-Carbon Technol 8(1):1–6. https://doi.org/10.1093/ijlct/cts001

Rodriguez C, Laplace P, Gallach-Perez D, Pellacani P, Martín-Palma RJ, Torres-Costa V, Ceccone G, Silván MM (2016) Hydrophobic perfluoro-silane functionalization of porous silicon photoluminescent films and particles. Appl Surf Sci 380:243–248. https://doi.org/10.1016/j.apsusc.2016.01.119

Rosenthal M, Bues CT (2010) Longitudinal infiltration of silicon dioxide nanosols in wood of *Pinus sylvestris*. Eur J Wood Prod 68(3):363–366. https://doi.org/10.1007/s00107-010-0455-5

Sahin HT, Mantanis GI (2011) Nano-based surface treatment effects on swelling, water sorption and hardness of wood. Maderas-Cienc Tecnol 13(1):41–48. https://doi.org/10.4067/S0718-221X2011000100004

Saka S, Ueno T (1997) Several SiO_2 wood–inorganic composites and their fire-resisting properties. Wood Sci Technol 31(6):457–466. https://doi.org/10.1007/BF00702568

Saka S, Sasaki M, Tanahashi M (1992) Wood–inorganic composites prepared by sol-gel processing. 1. Wood–inorganic composites with porous structure. Mokuzai Gakkaishi 38:1043–1104

Saka S, Miyafuji H, Tanno F (2001) Sol-gel products news. J Sol-Gel Sci Techn 20:213–217. https://doi.org/10.1023/A:1017330925894

Schwanninger M, Rodrigues JC, Fackler K (2011) A review of band assignments in near infrared spectra of wood and wood components. J near Infrared Spectrosc 19:287–308. https://doi.org/10.1255/jnirs.955

Sedighi Gilani M, Boone MN, Fife JL, Zhao SH, Koebel MM, Zimmermann T, Tingaut P (2016a) Structure of cellulose: silica hybrid aerogel at sub-micron scale, studied by synchrotron X-ray tomographic microscopy. Compos Sci Technol 124:71–80. https://doi.org/10.1016/j.compscitech.2016.01.013

Sedighi Gilani M, Zhao S, Gaan S, Koebel MM, Zimmermann T (2016b) Design of a hierarchically structured hybrid material: via in situ assembly of a silica aerogel into a wood cellular structure. RSC Adv 6:62825–62832. https://doi.org/10.1039/C6RA12480A

Shabir Mahr M, Hübert T, Schartel B, Bahr H, Sabel M, Militz H (2012) Fire retardancy effects in single and double layered sol–gel derived TiO_2 and SiO_2-wood composites. J Sol-Gel Sci Techn 64(2):452–464. https://doi.org/10.1007/s10971-012-2877-5

Skaar C (1988) Hygroexpansion in wood. In: Timell TE (ed) Wood-water relations. Springer, Berlin, pp 122–176

Terziev N, Panov D, Temiz A, Palanti S, Feci E, Daniel G (2009) Laboratory and above ground exposure efficacy of silicon-boron treatments. IRG/WP 09-30510.

Tshabalala MA, Kingshott P, VanLandingham MR, Plackett D (2003) Surface chemistry and moisture sorption properties of wood coated with multifunctional alkoxysilanes by sol-gel process. J Appl Polym Sci 88(12):2828–2841. https://doi.org/10.1007/BF02730098

Unger B, Bücker M, Reinsch S, Hübert T (2013) Chemical aspects of wood modification by sol–gel-derived silica. Wood Sci Technol 47(1):83–104. https://doi.org/10.1007/s00226-012-0486-7

Veres P, Kéri M, Bányai I, Lázár I, Fábián I, Domingo C, Kalmár J (2017) Mechanism of drug release from silica-gelatin aerogel: relationship between matrix structure and release kinetics. Colloid Surface B 152:229–237. https://doi.org/10.1016/j.colsurfb.2017.01.019

Wagenführ R (1996) Holzatlas. Carl Hanser Verlag, München, pp 213–397

Wang S, Mahlberg R, Jämsä S, Nikkola J, Mannila J, Ritschkoff A-C, Peltonen J (2011) Surface properties and moisture behaviour of pine and heat-treated spruce modified with alkoxysilanes by sol–gel process. Prog Org Coat 71(3):274–282. https://doi.org/10.1016/j.porgcoat.2011.03.011

Wang X, Chai Y, Liu J (2013) Formation of highly hydrophobic wood surfaces using silica nanoparticles modified with long-chain alkylsilane. Holzforschung 67:667–672. https://doi.org/10.1515/hf-2012-0153

Xu E, Zhang Y, Lin L (2020) Improvement of Mechanical, hydrophobicity and thermal properties of Chinese fir wood by impregnation of nano silica sol. Polymers 12(8):1632. https://doi.org/10.3390/polym12081632

Yu X, Sun D, Li X (2011) Preparation and characterization of urea-formaldehyde resin-sodium montmorillonite intercalation-modified poplar. J Wood Sci 57(6):501–506. https://doi.org/10.1007/s10086-011-1203-0

Yue D, Feng Q, Huang X, Zhang X, Chen H (2019) In situ fabrication of a superhydrophobic ormosil coating on wood by an ammonia–HMDS vapor treatment. Coatings 9:556. https://doi.org/10.3390/coatings9090556

Zeng Q, Mao T, Li H, Peng Y (2018) Thermally insulating lightweight cement-based composites incorporating glass beads and nanosilica aerogels for sustainably energy-saving buildings. Energy Build 174:97–110. https://doi.org/10.1016/j.enbuild.2018.06.031

Zhao S, Zhang Z, Sebe G, Wu R, Rivera Virtudazo RV, Tingaut P, Koebel MM (2015) Multiscale assembly of superinsulating silica aerogels within silylated nanocellulosic scaffolds: improved mechanical properties promoted by nanoscale chemical compatibilization. Adv Funct Mater 25(15):2326–2334. https://doi.org/10.1002/adfm.201404368

Zhu X, Wu Y, Tian C, Qing Y, Yao CH (2014) Synergistic effect of nanosilica aerogel with phosphorus flame retardants on improving flame retardancy and leaching resistance of wood. J Nanomater. https://doi.org/10.1155/2014/867106